An enhanced CMM model to predict CVT performances: theory vs. experiment

Giuseppe Carbone[1], Leonardo De Novellis[1], Luigi Mangialardi[1]
[1]*Dipartimento di Ingegneria Meccanica e Gestionale, Politecnico di Bari, Italy*
E-mail: g.carbone@poliba.it, l.denovellis@poliba.it, lmm@poliba.it

Keywords: Continuously variable transmission, chain drive, traction performances.

SUMMARY. The paper deals with the theoretical and experimental evaluation of the performance of a CVT chain drive in steady state conditions. We propose an enhanced version of the CMM model, to accurately predict the slip behaviour and the traction performance of the variator. We show that to achieve this objective it is necessary to accurately describe the elastic displacements of the pulley. Indeed, this allows also to accurately predict the sliding velocities at the pin-pulley interface and, therefore, the total slip and the traction performance of the variator. A comparison between the theoretical predictions and the experimental measurements is also presented, which shows a good agreement between theory and experiments.

1 INTRODUCTION

Nowadays a great deal of research is being carried out to achieve a reduction of fuel consumptions and polluting emissions of engine cars, and guarantee improved comfort and driveability. The continuously variable transmission (CVT) may represent a promising attempt to conciliate these requirements of the modern automotive market [1, 2, 3, 4]. However, for the sake of design and control purposes, modelling CVT dynamical behavior plays a fundamental role [5, 6, 7, 8, 9, 10, 11, 12, 13]. A correct modelling of the variator allows, indeed, to understand what are the main physical, geometrical and mechanical parameters that must be tuned to achieve optimal CVT performance. This is even more true for high torque CVTs, which, in the last few years, are being designed and manufactured to equip big engine cars. Different typologies have been developed, but among these the Gear Chain Industrial (GCI) chain CVT (see Fig. 1) gained high interest for its low manufacturing costs and because it offers the possibility to easily scale the chain design for extremely high torque applications [14].

A new theoretical model (the so called CMM model) has been proposed in Ref. [5] to describe belt and/or chain CVT dynamics giving reliable predictions during CVT shifting manouvers [15]. In this paper we present a further refinement of the model: the elastic deformation have been calculated by employing a Green function approach. In contrast with the multibody characterization of the chain proposed by other authors [10], the new approach has a very simple formulation and results in a easy implementation, that makes this model suitable for a complete and fast evaluation of the variator working points. In this work we focus on the modelling of a CVT chain transmission in steady state, and we show a critical comparison between theoretical calculations and experimental measurements. In particular, the evaluation of the steady state performances is carried out through the analysis of the thrust forces ratio necessary to achieve the desired transmission ratio and through the evaluation of the traction capabilities, namely the estimation of the traction coefficient μ as a function of the overall slip σ of the variator.

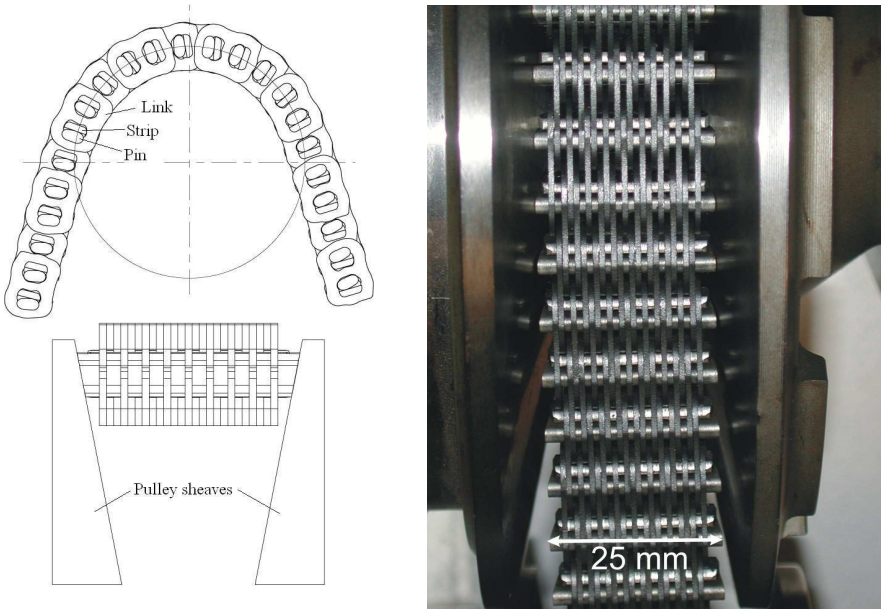

(a) (b)

Figure 1: Components of the GCI chain with the links and the conjugate profiles (pins and strips) which are useful for reducing the polygonal effect.

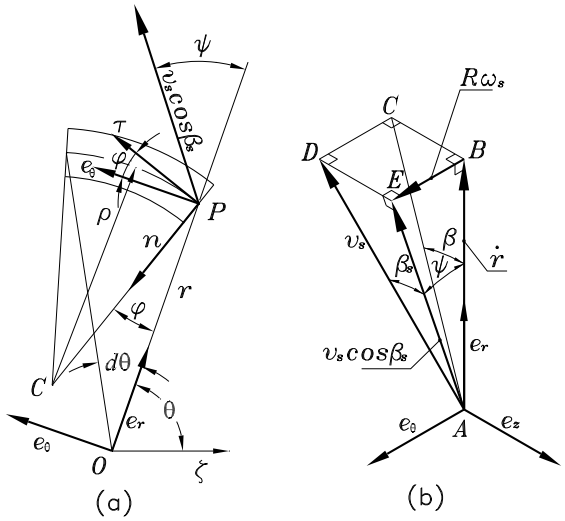

Figure 2: Kinematic and geometric quantities.

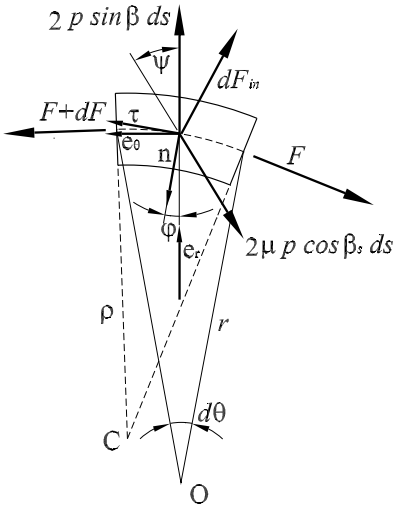

Figure 3: The forces acting on the chain.

2 THE CHAIN DRIVE MODEL

The model of the metal chain is based on the CMM model [5], which treats the chain as a one-dimensional continuum body having a locally rigid motion. Since the longitudinal elongation of the chain is neglected, the mass conservation law equation can be written as

$$v_r + \frac{\partial v_\theta}{\partial \theta} = 0 \tag{1}$$

where $v_r = \dot{r}$ and v_θ are the radial and tangential sliding velocity of the chain respectively, as depicted in Fig. 2. The quantity r is the local radial position of the chain. The radial velocity of the chain is related to the pulley deformation and it can be evaluated by means of the Sattler's approximation of the pulley bending [16] which leads to the following formulation of v_r in steady state condition as

$$v_r = a\Delta\omega R \sin(\theta - \theta_c) \tag{2}$$

where R is the chain pitch radius, Δ is the peak amplitude of the deformed sheave angle and $a = (1 + \cos^2\beta_0)/\sin(2\beta_0)$, where β_0 is the half-groove angle of the pulleys. The quantity θ is the angular coordinate and θ_c is the centre of the wedge expansion which can be estimated as

$$\tan\theta_c = \frac{\int_0^\alpha p(\theta)\sin\theta d\theta}{\int_0^\alpha p(\theta)\cos\theta d\theta} \tag{3}$$

where p is the linear pressure (force per unit longitudinal chain length) acting at the pin-pulley interface, and α is the angular extension of the contact arc. By means of FEM calculations performed on a detailed model of the CVT variator employed for the experiments, the deflection parameter Δ has been evaluated depending on the pressure distribution p with a Green's function approach. Our calculations show that the groove angle can be expressed as

$$\beta - \beta_0 = \Gamma + 0.5\Delta\cos(\theta - \theta_c) \tag{4}$$

where the terms Γ and Δ are function of the clamping force S and of the transmission ratio τ only, i.e.

$$\Gamma = \Gamma(\tau, S) \tag{5}$$

$$\Delta = \Delta(\tau, S) \tag{6}$$

As an example of calculation, at $\tau = 1$ and $S = 4$kN we obtained $\Delta = 0.2$mrad and $\Gamma = 0.02$mrad, while, for an increased value of the clamping force $S = 30$kN, the deflection parameters become respectively $\Delta = 1.5$mrad and $\Gamma = 0.24$mrad.

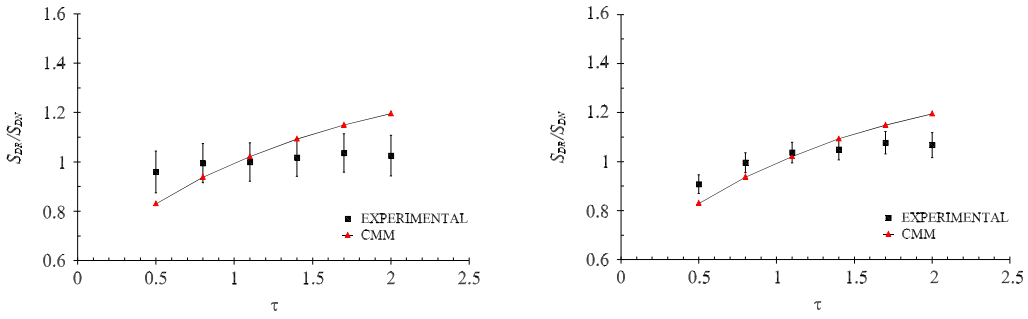

(a) $S_{DN} = 5$kN

(b) $S_{DN} = 10$kN

(c) $S_{DN} = 15$kN

(d) $S_{DN} = 20$kN

Figure 4: Clamping force ratio as a function of the the speed ratio τ, for a primary torque $T_{DR} = 0$Nm.

The equilibrium of the chain (see Fig. 3) involves the tension F, the pressure per unit chain length p, the inertia force of the chain element and the friction forces

$$\frac{1}{F - m\omega^2 R^2} \frac{\partial (F - m\omega^2 R^2)}{\partial \theta} = \frac{\mu \cos \beta_s \sin \psi}{\sin \beta_0 - \mu \cos \beta_s \cos \psi} \tag{7}$$

$$p = \frac{F - m\omega^2 R^2}{2R(\sin \beta_0 - \mu \cos \beta_s \cos \psi)} \tag{8}$$

where m is the mass per unit length of the chain, ω the angular speed of the pulley, μ the local friction coefficient between the pin and the pulley and β_0 the half-groove angle of the undeformed

pulley. The quantity ψ is the sliding angle and is related to the radial and tangential velocity through the relation

$$\tan\psi = \frac{v_\theta}{v_r} \tag{9}$$

In order to evaluate the performances of the whole variator, in steady state, we can couple the pulleys by means of the proper coupling equations, which are

$$\begin{aligned} (v_{out})_{DR} &= (v_{in})_{DN} \\ (F_{out})_{DR} &= (F_{in})_{DN} \\ (F_{in})_{DR} &= (F_{out})_{DN} \end{aligned} \tag{10}$$

where the subscript DR refers to the primary pulley (drive) and the subscript DN to the secondary (driven) one. The quantities v_{out} and v_{in} are the absolute chain velocities at the output and input points of the wrap arc. The local absolute velocity of the chain is $v = [v_r^2 + (v_\theta + r\omega)^2]^{1/2}$.

3 THEORETICAL-EXPERIMENTAL COMPARISON

Experimental measurements have been carried out on a chain CVT by Gear Chain Industrial (GCI B.V.) for validation.

The CVT transmission employed during the experiments is mounted on the Power Loop Test Rig available at the Automotive and Engineering Science laboratory at the Technische Universiteit Eindhoven and it is characterized by the following data: belt length $L = 703$mm, centre-to-centre distance of the pulleys $i = 168$mm, undeformed sheave angle $\beta_0 = 11$deg. The friction coefficient has been considered equal to $\mu = 0.09$.

3.1 *Thrust force ratio*

The clamping forces experiments have been carried out by fixing the speed ω_{DR} and the torque T_{DR} of the drive pulley and the clamping force acting on the driven movable sheave S_{DN}. The relation $S = pA + F_c$ has been employed to evaluate the clamping force by considering that p is the oil pressure, A is the pressurized area of the movable sheave and F_c is the centrifugal term which is function of the oil density ρ, of the pulley angular velocity ω and of the minimum radius r_1 and maximum radius r_2 of the hydraulic chamber. As suggested by the manufacturer of such system, the centrifugal term F_c is estimated through the formula $F_c = \pi\rho\omega^2(r_2^4 - r_1^4)/4$.

Figure 4 shows the clamping force ratio at zero torque load and primary speed $\omega_{DR} = 2000\mathrm{RPM}$ and for four different secondary clamping forces ($S_{DN} = 5, 10, 15, 20\,\mathrm{kN}$). The agreement between theory and the experimental data is very good at higher values of the secondary clamping force, [see Figs. 4(c)-(d)], while at low clamping force level there is a significant divergence as shown in Fig. 4(a)-(b) where the experimental data present a flat trend in contrast with the theoretical values, which show a monotonic behaviour. This tendency is confirmed at a higher value of the torque load ($T_{DR} = 30\mathrm{Nm}$) where we notice a very good agreement at high clamping forces [see Figs. 5(c)-(d)].

We think indeed that at high thrust force ratios the predictions of the theoretical model match very well the experimental measurements; furthermore, at low values of the secondary clamping force the influence of secondary effects, which actually are neglected by the theoretical model, have a strong influence on the measured data, determining the divergence between the theoretical curve and the experimental one. These secondary effects should be independent of the speed ratio τ and secondary clamping force S_{DN}, and may be related to friction in the crank spindle joint or to friction in the seals of the primary and secondary hydraulic cylinders.

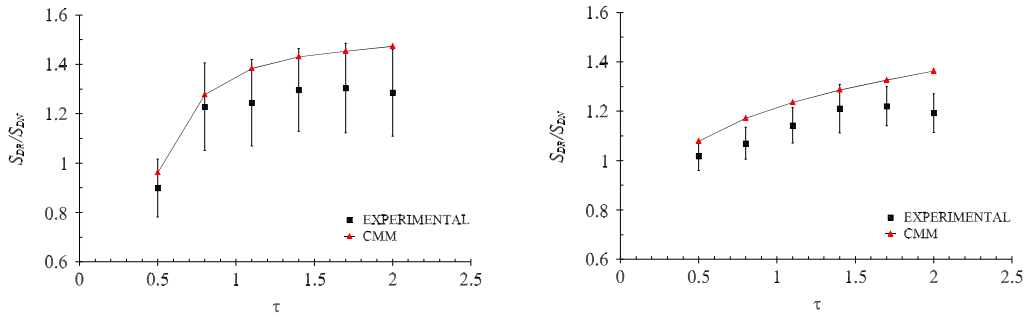

(a) $S_{DN} = 5$kN (b) $S_{DN} = 10$kN

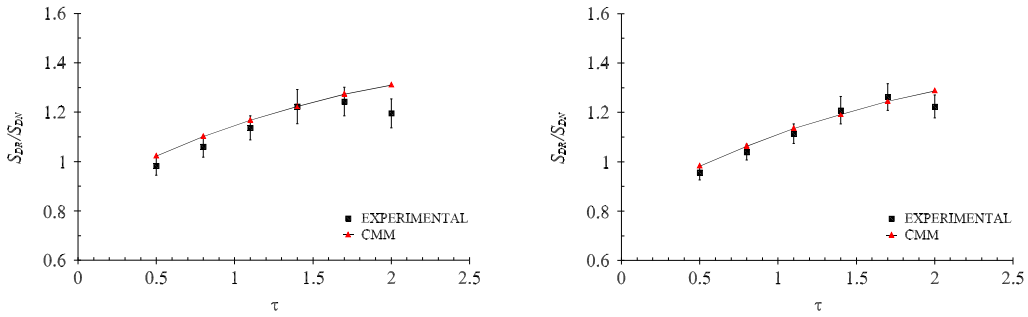

(c) $S_{DN} = 15$kN (d) $S_{DN} = 20$kN

Figure 5: Clamping force ratio as a function of the the speed ratio τ, for a primary torque $T_{DR} = 30$Nm.

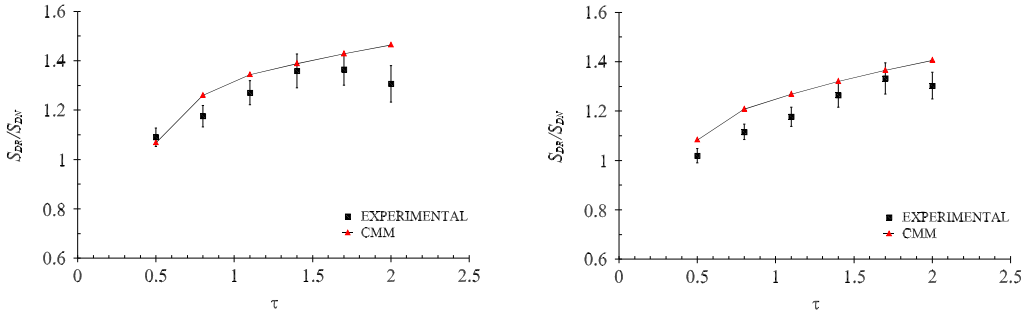

(a) $S_{DN} = 15$kN (b) $S_{DN} = 20$kN

Figure 6: Clamping force ratio as a function of the the speed ratio τ, for a primary torque $T_{DR} = 70$Nm.

At higher torque values (see Fig. 6), larger clamping forces are needed to guarantee the power transmissions. For this reason the experimental curves are shifted towards higher values of the clamping force ratios. We observe that also in this case the agreement with the theoretical predictions is still very good with a difference limited to less than 5% at $\tau = 0.7$ and $S_{DN} = 20\text{kN}$ [see Fig. 6 (b)].

3.2 *Traction performances*

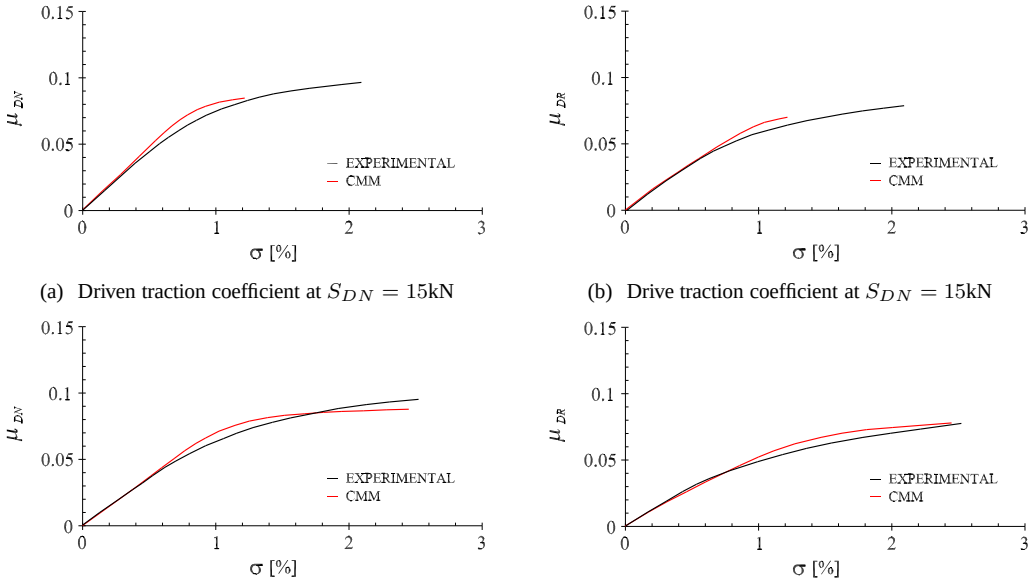

(a) Driven traction coefficient at $S_{DN} = 15\text{kN}$

(b) Drive traction coefficient at $S_{DN} = 15\text{kN}$

(c) Driven traction coefficient at $S_{DN} = 20\text{kN}$

(d) Drive traction coefficient at $S_{DN} = 20\text{kN}$

Figure 7: Comparison between the traction coefficient on the drive pulley evaluated with the CMM model and the measured one during a traction test performed at transmission ratio $\tau_{id} = 1$, $\omega_{DR} = 500\text{RPM}$ as primary speed and different secondary clamping forces.

The traction properties of the CVT variators are usually described by means of the evaluation of the traction coefficients μ and of the overall slip σ of the variator, which are defined as

$$\mu_{DR} = \frac{T_{DR} \cos \beta_0}{2 R_{DR} S_{DR}} \tag{11}$$

$$\mu_{DN} = \frac{T_{DN} \cos \beta_0}{2 R_{DN} S_{DN}} \tag{12}$$

$$\sigma = \frac{\omega_{DR} R_{DR} - \omega_{DN} R_{DN}}{\omega_{DR} R_{DR}} \tag{13}$$

where T is the torque, R is the pitch radius, S stands for the clamping force, ω is the shaft angular velocity and β_0 is the undeformed sheave angle. Furthermore, the subscript DR refers to the drive pulley (i.e. the primary pulley) and the subscript DN refers to the driven pulley.

The experimental evaluation of the traction coefficient as a function of the overall slip of the chain drive has been performed for the unit geometric ratio $\tau_{id} = R_{DR}/R_{DN}$ at a fixed value of the primary speed ω_{DR} and secondary clamping force S_{DN} while increasing the primary torque up to the limit traction value. The results of the traction tests have been compared with the theoretical traction curves calculated with the enhanced CMM model. As shown in Figure 7(a)-(b), at a value of the secondary clamping force $S_{DN} = 15\mathrm{kN}$ and primary pulley speed $\omega_{DR} = 500\mathrm{RPM}$ there is a good agreement between theoretical predictions and experiments in the linear part of the traction curve (the so-called microslip region).

The influence of the pulley deformation on the variator traction behaviour is evident when the traction tests are carried out at higher values of the thrust forces: at $S_{DN} = 20\mathrm{kN}$ [see Fig. 7(c)-(d)] the slope of the measured curve in the microslip region is considerably reduced when compared with the test at $S_{DN} = 15\mathrm{kN}$. Furthermore, we point out a closer match between theory and experiments, in these working conditions, both on the primary and secondary pulley. In all the examined cases, we observed the presence of a limit slip value which represents the transition between the microslip and the macroslip region. The value of $\sigma_T = 1\%$, indeed, can be interpreted as the threshold, for the chain drive, beyond which macroscopic slip occurs.

4 CONCLUSIONS

We have presented an enhanced version of the CMM model by including a more accurate description of the elastic pulley bending. We have also investigated the reliability of the improved model with a theoretical-experimental comparison of a chain drive variator in steady state conditions. Our calculations have shown a good agreement between theory and experiments especially at high clamping forces values, either in predicting the thrust force ratio necessary to establish the desired transmission ratio either in evaluating the variator traction behaviour.

Moreover, with our measurements we have remarked the influence of the pulley deformation on the sliding velocities at the chain pin-pulley interface, leading to consistent differences in the slope of the traction curve in the microslip region, when the traction tests are carried out at different clamping force values. The enhanced CMM model is indeed capable to describe such experimental evidence which actually makes the presented model unique in the evaluation of the performances of a CVT variator. This feature of the model together with its very low computational cost makes it a very useful tool during the design process of this kind of variators.

References

[1] Mantriota G., "Fuel consumption of a vehicle with power split CVT system," *Int. J. Veh. Des.*, **37**, 327-342 (2005).

[2] Brace C., Deacon M., Vaughan N. D., Horrocks R. W. and Burrows C. R., "The Compromise in Reducing Exhaust Emissions and Fuel Consumption from a Diesel CVT Powertrain over Typical Usage Cycles," in *Proc. Int. Congress on Continuously Variable Power Transmission CVT?99*, Eindhoven, The Netherlands, September 16?17, 1999, 27-33 (1999).

[3] Brace C., Deacon M., Vaughan N. D., Burrows C. R. and Horrocks R. W., "Integrated passenger cat diesel CVT powertrain control for economy and low emissions," in *ImechE International Seminar S540 'Advanced Vehicle Transmission and Powertrain Management'*, September 25-26, (1997).

[4] Carbone G., Mangialardi L. and Mantriota G., "Fuel Consumption of a Mid Class Vehicle with Infinitely Variable Transmission," *SAE J. Engines*, **110**, 2474-2483 (2002).

[5] Carbone G. Mangialardi L. and Mantriota G., "The influence of pulley deformations on the shifting mechanisms of MVB-CVT," *J. Mech. Des.*, **127**, 103-113 (2005).

[6] Kanehara S., Fujii T. and Kitagawa T., "A study of a Metal Pushing V-Belt type CVT - Part 3: What Forces Act on Metal Blocks?," *SAE paper 940735*, (1994).

[7] Micklem J.D., Longmore D.K. and Burrows C.R., "Modelling of the steel pushing V-belt continuously variable transmission," *J. Mech. Eng. Sci.*, **208**, 13-27 (1994).

[8] Srivastava N. and Haque I., "Clearance and friction induced dynamics of chain CVT drives," *Multibody Syst. Dyn.*, **19**, 255-280 (2008).

[9] Sorge F., "Influence of pulley bending on metal V-belt mechanics," in *Proc. Int. Conference on Continuously Variable Power Transmission, Japanese Society of Automotive Engineers, Paper No. 102 (9636268)*, Yokohama, Japan, September 11-12, 9-15 (1996).

[10] Srnik J. and Pfeiffer F., "Dynamics of CVT Chain Drives," *Int. J. Veh. Des.*, **22**, 54-72 (1999).

[11] Ide T., Udagawa A. and Kataoka R., "Simulation Approach to the Effect of the Ratio Changing Speed of a Metal V-Belt CVT on the Vehicle Response," *Veh. Syst. Dyn.*, **24**, 377-388 (1995).

[12] Carbone G., Mangialardi L. and Mantriota G., "Theoretical model of metal V-Belt drives during rapid ratio changing," *J. Mech. Des.*, **123**, 111-117 (2001).

[13] Carbone G., Mangialardi L. and Mantriota G., "Influence of Clearance Between Plates in Metal Pushing V-Belt Dynamics," *J. Mech. Des.*, **124**, 543-557 (2002).

[14] van Rooij J. and Frank A.A., "Development of a 700Nm chain CVT," in *Proc. Int. Congress on Continuously Variable Transmission* (VDI Berichte 1709), Munich, Germany, 179-194 (2002).

[15] Carbone G., Mangialardi L., Bonsen B., Tursi C. and Veenhuizen P.A., "CVT Dynamics: Theory and experiments," *Mech. Mach. Theory*, **42**, 409-428 (2007).

[16] Sattler H., "Efficiency of Metal Chain and V-Belt CVT," in *Proc. Int. Congress on Continuously Variable Power Transmission CVT?99*, Eindhoven, The Netherlands, September 16?17, 1999, 99-104 (1999).